Novel Organic Ions of High-Spin States. 2. Determination of the Spin Multiplicity of the Ground State and ^{1}H-ENDOR Study of the Monoanion of *m*-Phenylenebis(phenylmethylene)

Michio Matsushita,[†] Toshihiro Nakamura,[†] Takamasa Momose,[†] Tadamasa Shida,*[,†] Yoshio Teki,[‡] Takeji Takui,[‡] Takamasa Kinoshita,[‡] and Koichi Itoh*[,‡]

Contribution from the Department of Chemistry, Faculty of Science, Kyoto University, Kyoto 606-01, Japan, and Department of Chemistry, Faculty of Science, Osaka City University, Sugimoto, Sumiyoshi-ku, Osaka 558, Japan. *Received February 13, 1992*

Abstract: ESR and ^{1}H-ENDOR measurements of the title anion were performed at temperatures below 4 K. From the temperature dependence of the intensity of the ESR signal the spin multiplicity of the anion in the ground state was concluded to be quartet. The ^{1}H-ENDOR measurement was carried out for the randomly oriented sample by monitoring the *X*- and *Y*-axis canonical peaks and the off-axis extra line. From the hyperfine coupling constants (hfcc) of the protons and the divalent ^{13}C atoms it was concluded that the excess electron in the anion occupies one of the two nonbonding π-orbitals. The molecular conformation of the anion was suggested to be trans-trans in contrast to cis-trans for the neutral *m*-phenylenebis(phenylmethylene).

Introduction

Aromatic high-spin polycarbenes[1,2] have been receiving continuous interest as models for organic superparamagnets or ferromagnets.[3-11] The spin alignment of aromatic polycarbenes in their ground state can be predicted by the topology of the π-electron network.[12,21] However, as for charged polycarbenes being a novel class of high-spin molecules, there is no such simple guiding principle, though a theoretical prediction was made on the possible reversal of the order of high- and low-spin states upon ionization.[22] As the first example of charged high-spin polycarbenes, we have reported the monoanion of *m*-phenylenebis(phenylmethylene) (*m*-PBPM).[23,24] Charged high-spin molecules are suitable systems for studying the correlation between the charge and the spin in organic systems.

In the present work, ESR measurements of the anion at temperatures below 4 K were performed. From the temperature dependence of the intensity of the ESR signal the ground state of the monoanion was determined to be quartet. In order to characterize the electronic structure we have performed ^{1}H-ENDOR measurements. ESR measurements of the ^{13}C substituted isotopomer were also made to obtain the spin density at the divalent carbon atoms.

Experimental Section

The quartet anion was formed as in the previous work by the electron attachment to the corresponding diazo precursor, 1,3-bis(α-diazobenzyl)benzene (1,3-BDB), followed by denitrogenation by visible light.[23,24] Since not all the 1,3-BDB was converted to its anion, the neutral *m*-PBPM could also be produced by UV photolysis of the remaining 1,3-BDB.[1,2] The ESR signal of *m*-PBPM thus produced was used as an internal standard of the temperature. In order to avoid the artifact due to the instrumental difference, ESR experiments were performed using both a JEOL PE-2X spectrometer with an Air Products LTR-3 refrigerator and a Bruker ESP 300 spectrometer with an Oxford ESR 910 temperature controller. Also, in order to avoid the power saturation at low temperatures, the microwave power was attenuated to 0.02-0.04 μW in the JEOL spectrometer equipped with a cylindrical TE_{011} cavity and to 0.2 μW in the Bruker spectrometer with a rectangular TE_{102} cavity.

^{1}H-ENDOR measurements were carried out with a Bruker ESP 300/350 spectrometer equipped with the Oxford ESR 910 temperature controller.

The ^{13}C labeled diazo precursor, 1,3-bis(α-[^{13}C]diazobenzyl)benzene, was synthesized with benzoic-α-^{13}C acid (99 atom % ^{13}C, Aldrich Chemical Company Inc., Milwaukee, Wisconsin) as a starting material via the following sequence of reactions (see Scheme I): chlorination with the thionyl chloride of ^{13}C labeled benzoic acid, Grignard coupling with 3-bromodiphenylmethane (74% yield), oxidation with chromium trioxide in acetic acid-acetic anhydride (83% yield, mp 107-108 °C), condensation with hydrazine hydrate in ethanol (55% yield, mp 166-168 °C), and oxidation with activated manganese dioxide in dichloromethane (60%

Scheme I. Preparation of the ^{13}C Labeled Diazo Precursor[a]

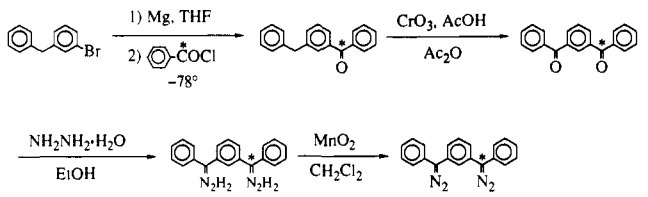

[a] Asterisks denote ^{13}C.

(1) Itoh, K. *Chem. Phys. Lett.* **1967**, *1*, 235-238.
(2) Wasserman, E.; Murray, R. W.; Yager, W. A.; Trozzolo, A. M.; Smolinsky, G. *J. Am. Chem. Soc.* **1967**, *89*, 5076-5078.
(3) For a recent overview, see: *Proceedings of the Symposium on Ferromagnetic and High-Spin Molecular Based Material*, 197th National Meeting of the American Chemical Society, Dallas, TX, April, 1989; American Chemical Society: Washington, DC. Miller, J. S., Doughterty, D. A., Eds. *Mol. Cryst. Liq. Cryst.* **1989**, *176*, pp 1-562. *Materials Research Society Symposium Proceedings*, Vol. 173. *Advanced Organic Solid State Materials*; Chiang, L. Y., Chaikin, P. M., Cowan, D. O., Eds.; Materials Research Society: Pittsburgh, PA, 1989; pp 3-92. *Molecular Magnetic Materials*; Gatteschi, D., Kahn, O., Miller, J. S. *Palacio*, F., Eds.; Kluwer Academic: Dordrecht, 1991; Vol. A198.
(4) Kaisaki, D. A.; Chang, W.; Dougherty, D. A. *J. Am. Chem. Soc.* **1991**, *113*, 2764-2766. Dougherty, D. A. *Acc. Chem. Res.* **1991**, *24*, 88-94.
(5) Rajca, A. *J. Am. Chem. Soc.* **1990**, *112*, 5889-5890. Rajca, A. *J. Am. Chem. Soc.* **1990**, *112*, 5890-5892. Rajca, A.; Utamapanya, S.; Xu, J. *J. Am. Chem. Soc.* **1991**, *113*, 9235-9241. Utamapanya, S.; Rajca, A. *J. Am. Chem. Soc.* **1991**, *113*, 9242-9251.
(6) Kinoshita, M.; Turek, P.; Tamura, M.; Nozawa, K.; Shiomi, D.; Nakazawa, Y.; Ishikawa, M.; Takahashi, M.; Awaga, K.; Inabe, T.; Maruyama, Y. *Chem. Lett.* **1991**, 1225-1228. Takahashi, M.; Turek, P.; Nakazawa, Y.; Tamura, M.; Nozawa, K.; Shiomi, D.; Ishikawa, M.; Kinoshita, M. *Phys. Rev. Lett.* **1991**, *67*, 746-748.
(7) Allemand, P. M.; Khemani, K. C.; Koch, A.; Wudl, F.; Holczer, K.; Donovan, S.; Grüner, G.; Thompson, J. D. *Science* **1991**, *253*, 301-303.
(8) Kollmar, C.; Kahn, O. *J. Am. Chem. Soc.* **1991**, *113*, 7987-7994. Kollmar, C.; Couty, M.; Kahn, O. *J. Am. Chem. Soc.* **1991**, *113*, 7994-8005.
(9) Broderick, W. E.; Thompson, J. A.; Day, E. P.; Hoffman, B. M. *Science* **1990**, *249*, 401-403.
(10) Manriquez, J. M.; Yee, G. T.; McLean, R. S.; Epstein, A. J.; Miller, J. S. *Science* **1991**, *252*, 1415-1417. Yee, G. T.; Manriquez, J. M.; Dixon, D. A.; McLean, R. S.; Groski, D. M.; Flippen, R. B.; Narayan, K. S.; Epstein, A. J.; Miller, J. S. *Adv. Mater. (Weinheim, Fed. Repub. Ger.)* **1991**, *3*, 309-311.
(11) Veciana, J.; Rovira, C.; Crespo, M. I.; Armet, O.; Domingo, V. M.; Palacio, F. *J. Am. Chem. Soc.* **1991**, *113*, 2552-2561.
(12) Itoh, K. *Bussei* **1971**, *12*, 635-646.
(13) Itoh, K. *Pure Appl. Chem.* **1978**, *50*, 1251-1259.
(14) (a) Teki, Y.; Takui, T.; Itoh, K.; Iwamura, H.; Kobayashi, K. *J. Am. Chem. Soc.* **1983**, *105*, 3722-3723. (b) Teki, Y.; Takui, T.; Itoh, K.; Iwamura, H.; Kobayashi, K. *J. Am. Chem. Soc.* **1986**, *108*, 2147-2156.
(15) (a) Teki, Y.; Takui, T.; Konoshita, T.; Ichikawa, S.; Yagi, H.; Itoh, K. *Chem. Phys. Lett.* **1987**, *141*, 201-205. (b) Teki, Y.; Takui, T.; Kitano, M.; Itoh, K. *Chem. Phys. Lett.* **1987**, *142*, 181-186.

[†] Kyoto University.
[‡] Osaka City University.

0002-7863/92/1514-7470$03.00/0

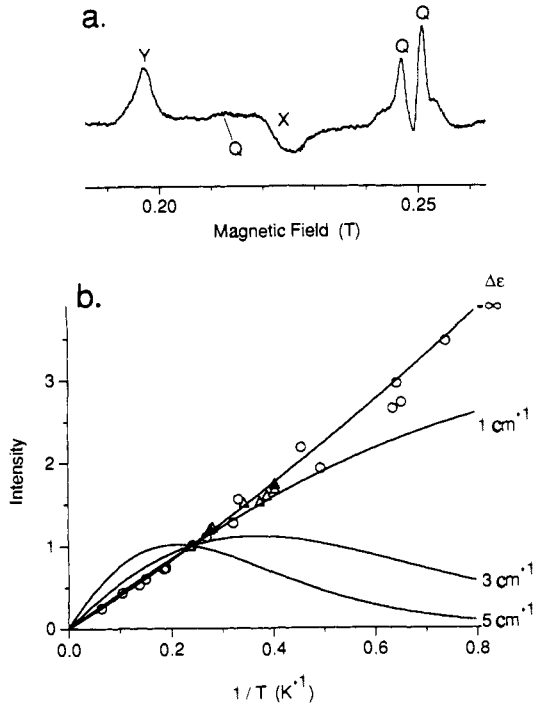

Figure 1. (a) Typical ESR spectrum used for the calculation of the temperature dependence of the intensity of the *Y*-axis canonical peak of the quartet anion. The signals due to the neutral quintet *m*-PBPM are indicated by Q. The temperature was calibrated by the intensity of the quintet signal at ≈0.25 T. The symbols X and Y denote the *X*- and *Y*-axis canonical peaks of the quartet anion. (b) Temperature dependence of the intensity of the ESR signal of the *Y*-axis canonical peak shown in the upper spectrum. The triangles are experimental data measured with a JEOL spectrometer. Since the line shape of the peak does not change with temperature, the intensity was calculated by the first derivative peak height. The circles indicate the data measured with a Bruker spectrometer, and the intensity was calculated by double integration of the first derivative spectrum. The plots obtained by the double integration were almost the same as those obtained by the first derivative peak heights. Solid curves are the calculated temperature dependence for several values of $\Delta\epsilon = \epsilon(\text{quartet}) - \epsilon(\text{doublet})$. All the experimental and theoretical intensities are normalized at $T = 4.2$ K.

yield, mp 130.5–131.5 °C dec). All of the melting points were uncorrected.

Results and Discussion

1. Spin Multiplicity of the Ground State of *m*-PBPM$^{\bullet-}$. In the previous report[23] the spin multiplicity of the monoanion in the ground state was concluded to be doublet from the measurement of the ESR intensity down to 3 K with the use of a germanium sensor as a thermometer. There remained, however, a possibility that the temperatures of the sample and the thermometer were discrepant since the thermometer was not in direct contact with the sample. To eliminate this ambiguity the signal intensity of the quintet *m*-PBPM, which was produced by UV photolysis (see Experimental Section), was exploited as an internal standard of the temperature in the present work. It is well established that the quintet state is the ground state of *m*-PBPM with the first excited state being separated enough (the energy gap $\gg 300$ cm^{-1}), and the signal intensity of the quintet is well calibrated against the temperature.[1] The temperature was remeasured down to 1.4 K.

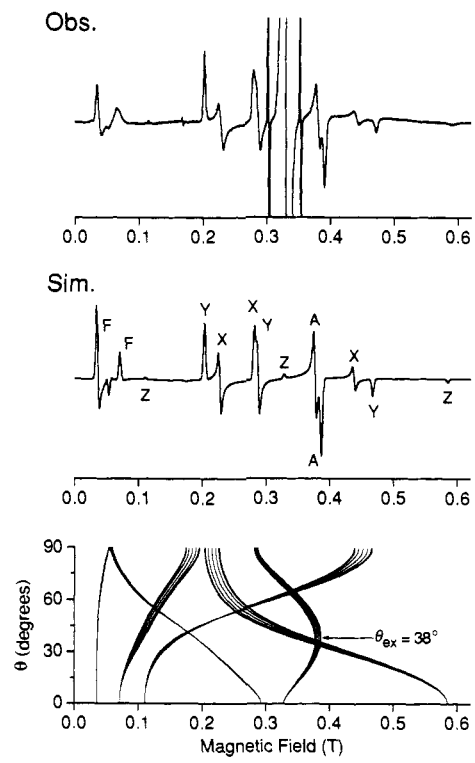

Figure 2. Observed and simulated X-band ESR spectra for the quartet state of *m*-PBPM$^{\bullet-}$. The angular dependence of resonant fields for the random orientation is shown at the bottom. Symbols A and F, respectively, denote the off-axis extra line[27] and the "forbidden" bands corresponding to the transitions with $\Delta m_S = \pm 2$ and ± 3. θ_{ex} denotes the angle corresponding to the extra line. The parameters used for the simulation are $\nu = 9.188$ GHz, $g = 2.003$ (isotropic), $D = +0.1200$ cm^{-1}, and $|E| = 0.0045$ cm^{-1}.[23]

Figure 1a shows a representative spectrum exhibiting the low-field *X*- and *Y*-axis canonical absorptions[25] of the anion along with several absorptions due to the quintet *m*-PBPM denoted by Q. The temperature dependence of the *Y*-axis peak of the anion obtained by the two instruments is shown in Figure 1b. The solid curves are calculated by considering the Boltzmann distribution in the sublevels of the quartet and the doublet states.[14b] The parameter $\Delta\epsilon$ denotes the energy gap of $\epsilon(\text{quartet}) - \epsilon(\text{doublet})$. The essentially linear plot fits the case of $\Delta\epsilon = -\infty$, which signifies $\epsilon(\text{quartet}) \ll \epsilon(\text{doublet})$. The possibility of $|\Delta\epsilon| < 1$ cm^{-1} can be ruled out by the following reasoning: if the energy gap is smaller than 1 cm^{-1}, the appreciable spin quantum mixing between the quartet and the doublet states should arise so that the eigenstate should not be described as a pure quartet or a pure doublet state. In such a case the resultant ESR spectrum should exhibit characteristic features such as the occurrence of new transitions and the shift of resonance fields from those for a pure quartet or a pure doublet state.[26] The spin quantum mixing is of rare occurrence, but once it does, crucial information on the potential and the modes of molecular and electronic structures can be obtained from the characteristic spectral feature in favorable cases. Since the present ESR spectrum can be analyzed unambiguously in terms of a pure quartet state,[23,24] the difference $|\Delta\epsilon|$ must be much larger than 1 cm^{-1} (see the simulation in Figure 2, which

(16) Alexander, S. A.; Klein, D. J. *J. Am. Chem. Soc.* **1988**, *110*, 3401–3405.
(17) Itoh, K.; Takui, T.; Teki, Y.; Kinoshita, T. *J. Mol. Electron.* **1988**, *4*, 181–186.
(18) Itoh, K.; Takui, T.; Teki, Y.; Kinoshita, T. *Mol. Cryst. Liq. Cryst.* **1989**, *176*, 49–65.
(19) Takui, T.; Kita, S.; Ichikawa, S.; Teki, Y.; Kinoshita, T.; Itoh, K. *Mol. Cryst. Liq. Cryst.* **1989**, *176*, 67–76.
(20) Fujita, I.; Teki, Y.; Takui, T.; Kinoshita, T.; Itoh, K.; Miko, F.; Sawaki, Y.; Iwamura, H.; Izuoka, A.; Sugawara, T. *J. Am. Chem. Soc.* **1990**, *112*, 4074–4075.
(21) Okamoto, M.; Teki, Y.; Takui, T.; Kinoshita, T.; Itoh, K. *Chem. Phys. Lett.* **1990**, *173*, 265–270.
(22) Yamaguchi, K.; Toyoda, Y.; Fueno, T. *Synth. Met.* **1987**, *19*, 81–86.
(23) Matsushita, M.; Momose, T.; Shida, T.; Teki, Y.; Takui, T.; Itoh, K. *J. Am. Chem. Soc.* **1990**, *112*, 4700–4702.
(24) Shida, T. *Annu. Rev. Phys. Chem.* **1991**, *42*, 55–81.
(25) For the sake of convenience the principal axis transitions X and Y are labeled under the assumption of $E > 0$.
(26) Takui, T. et al. Unpublished work.

was constructed on the assumption of $2S + 1 = 4$[23,24]). Thus, we conclude that the ground state of the monoanion is quartet contrary to the previous conclusion.[23] The convex curve of the signal intensity vs $1/T$ plot reported in the previous work[23] was found to be due to the saturation effect at a power of 0.6 μW of the JEOL spectrometer employed and to the underestimation of the temperature with the use of a germanium sensor. Since the germanium sensor was exposed to the helium gas flow directly, the temperature of the sensor must have been lower than that of the sample in the quartz cell in the previous work.[23]

2. Absolute Sign of the Fine Structure Parameter D for the Anion. The absolute sign of D can be determined by the effect of the thermal population in the sublevels of the quartet state upon the relative intensity of the ESR transitions. Since the lowest temperature in the previous work[23] was not low enough to disclose the significant effect, the temperature was lowered down to 1.4 K in the present work. The intensity of the high-field X-axis canonical absorption at ≈0.44 T was compared with that of the low-field one at ≈0.22 T (see Figure 2). The intensity of the absorption was calculated by double integration of the first derivative peaks. The high-field X absorption at 9.5 K is 1.9 times as strong as that at 1.4 K when normalized by the low-field X absorption. This result indicates unequivocally that the absolute signl of D is positive.

3. ^{1}H-ENDOR Spectra. In order to investigate the spin density distribution in the quartet ground state of the monoanion, ^{1}H-ENDOR measurements were carried out for the anion in the glassy solution of 2-methyltetrahydrofuran (MTHF) at 1.8 K.[23]

Since the ENDOR study of single-crystal samples provides the angular dependence of the hfcc, the principal values of the hyperfine coupled (hfc) tensor and the orientation of the principal axes relative to the crystal axes can be determined precisely. However, for a randomly oriented sample of high-spin molecules the ENDOR measurement is usually feasible only for the direction of the principal axes of the fine structure tensor because ESR lines in the first derivative mode correspond to the turning points, i.e., extremes of the angular dependence of the resonant field, which usually correspond to the direction of the principal axes of the tensor. In some cases, the angular dependence yields extra turning points at magnetic fields different from those corresponding to the principal axes. They give rise to off-axis extra lines in the powder-pattern spectrum[27] (see the angular dependence and the peak denoted by A in the simulated spectrum of Figure 2). In such a case it may be possible to observe the ENDOR signal corresponding to the extra turning point, which was indeed observed in the present study (see Figure 3d). In this context the reader is reminded that ENDOR signals can be observed, in principle, at any magnetic field if the ESR intensity and the condition of relaxation are favorable.

Let us briefly describe features of ^{1}H-ENDOR spectra for high-spin states. The ENDOR spectral pattern depends on the electron spin sublevels investigated; under the high-field approximation the ^{1}H-ENDOR frequency ν to first order is given by

$$\nu = |\nu_n - a m_S| \quad (1)$$

where ν_n is the Zeeman frequency of the free proton ($\nu_n > 0$) and the symbols a and $_{mS}$ denote the zz component of the hfc tensor expressed in frequency units and the magnetic quantum number of the electron spin, respectively. The direction of z is determined from the following equation: $z = \mathbf{g}\cdot\mathbf{h}/g$ where $\mathbf{g}$ and $\mathbf{h}$ denote the $\mathbf{g}$ tensor of the electron spin and the unit vector of the static magnetic field, respectively. For integral spin states, there are two characteristic ENDOR spectral patterns: one is that obtained by pumping the transition between $m_S = 0$ and ±1 sublevels. In this case all the signals due to the $m_S = 0$ state coalesce into a single peak at ν_n, and only the signals due to the $m_S = \pm 1$ state appear at frequencies apart from ν_n. Since the separation from ν_n gives $\pm a$, both the magnitude and relative sign of a of each proton can be directly determined from the spectrum (see Scheme IIa where a model system having two protons of $a_1 > 0$ and $a_2 < 0$ with $|a_1| > |\alpha_2|$ and $\nu_n > |am_S|$ is assumed). The other is associated with ESR transitions involving states of $m_S \neq 0$ and is more complicated than the former since the ENDOR signals due to both the upper and the lower electron spin sublevels appear at frequencies different from ν_n. The spectral resolution of the latter, however, is higher than that of the former because the separation of the ENDOR signals from ν_n is greater. Scheme IIb shows an example for the ESR transition between $m_S = 1$ and 2 sublevels. For half-integral spin states also, there are two characteristic ENDOR patterns: one is that obtained by monitoring the transition between $m_S = {}^1/_2$ and ${}^1/_2$ sublevels. In this case the ENDOR spectrum is symmetric with respect to ν_n, and a can be determined from the separation of the pair of the signals located symmetrically with respect to ν_n, though the sign of a cannot be determined from this spectrum (see Scheme IIc). The other pattern is asymmetric as is shown in Scheme IId for the transition between $m_S = {}^1/_2$ and ${}^3/_2$ sublevels. Since the proton having a gives two peaks at $\nu_n = 3/2a$ and $\nu_n - 1/2a$, both the magnitude and relative sign of a can be directly determined from the paired sets of the ENDOR signal in this case. It should be noted that ENDOR experiments afford us key information on the electron spin multiplicity of high-spin species under study, though the breakdown of the high-field approximation makes the spectral patterns more complicated than the simplified patterns as shown in Scheme II.

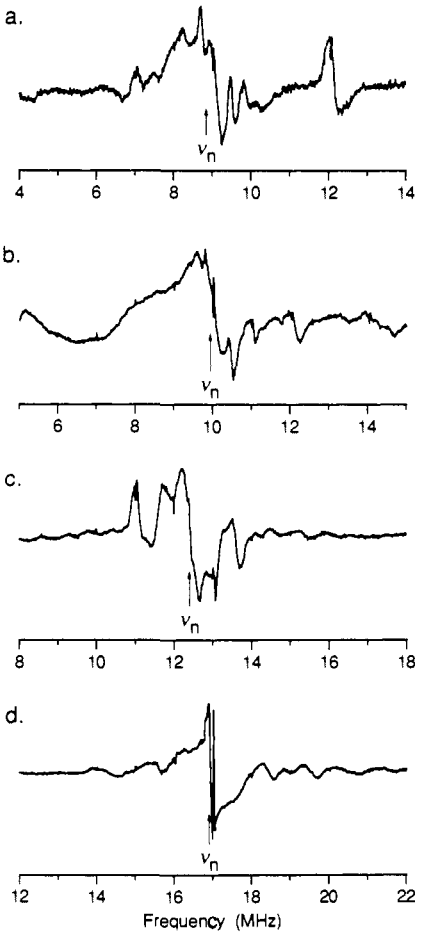

Figure 3. ^{1}H-ENDOR spectra of m-PBPM$^{\bullet-}$ in the glassy solution of 2-methyltetrahydrofuran (MTHF). The measurements were performed at 1.8 K. The magnetic field employed and the number of scans in each measurement were as follows: (a) 207.8 mT (Y-axis canonical peak of the transition from $m_S = -{}^3/_2$ to $-{}^1/_2$ sublevels) with 400 scans. (b) 233.3 mT (X-axis canonical peak of the transition from $m_S = -{}^3/_2$ to $-{}^1/_2$ sublevels) with 321 scans. (c) 291.3 mT (X- and Y-axis canonical peaks of the transition from $m_S = -{}^1/_2$ to ${}^1/_2$ sublevels) with 400 scans. (d) 397.0 mT (extra-line of the transition from $m_S = -{}^1/_2$ to ${}^1/_2$ sublevels) with 301 scans.

(27) Teki, Y.; Takui, T.; Itoh, K. *J. Chem. Phys.* **1988**, *88*, 6134–6145.

Scheme II. The Schematic Pattern of the ^{1}H-ENDOR Spectra of High-Spin States.[a]

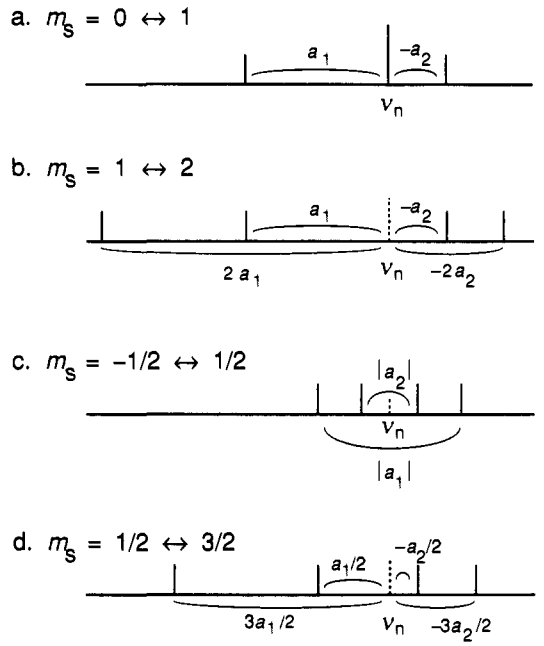

[a] A model system having two protons of $a_1 > 0$ and $a_2 < 0$ with $|a_1| > |a_2|$ and $\nu_n > |am_s|$ is assumed. The typical patterns for integral-spin states are shown in Scheme II parts a and b and those for half-integral spin states are shown in parts c and d. Scheme IIa, b, c, and d represents the patterns for the transitions between $m_s = 0$ and 1, 1 and 2, $-1/2$ and $1/2$, and $1/2$ and $3/2$, respectively.

The ^{1}H-ENDOR spectra of the monoanion were measured by monitoring the *X*- and *Y*-axis canonical peaks and the off-axis extra line denoted by A in Figure 2. The ENDOR signal corresponding to the *Z*-axis direction could not be detected because the ESR intensity was too weak. Figure 3 shows the ENDOR spectra observed from the four different ESR peaks. Since the ENDOR signals were weak, each spectrum was obtained by accumulating the signals over hundreds of scans. It should be noted that the ENDOR spectra obtained by monitoring ESR transitions between $m_S = -1/2$ and $1/2$ sublevels (Figure 3, parts c and d) are approximately symmetric with respect to ν_n in accordance with the explanation above. The ENDOR signals due to the individual 14 protons cannot be completely resolved. The inhomogeneous broadening of the ENDOR signals in the glassy solution is probably due to the failure of the selective pumping of a single molecular orientation and the statistical variation of the molecular conformation intrinsic to the glassy solution.[28] Therefore, we are focused to a semiquantitative argument in the following.

The neutral *m*-PBPM has four singly occupied molecular orbitals (SOMOs), two of which are the nonbonding π-orbitals and the other two are the in-plane nonbonding n-orbitals localized at the two divalent carbon atoms.[1,12,13] Therefore, the excess electron of the anion could occupy either the π- or the n-orbital. If it occupies the π-orbital, the spin density in the π-system will be half the magnitude of that of *m*-PBPM. On the other hand, if the excess electron resides on the n-orbital, the spin density of the π-electron system would be essentially unchanged but one of the n-orbitals is occupied by two electrons and the other remains singly occupied.

For the comparison of the hfcc of the quartet anion with the neutral quintet *m*-PBPM, the difference of the electron spin multiplicity must be taken into account. According to the projection theorem,[29] the hfc tensor of a state with the total electron spin angular momentum *S* contains the projection factor $1/(2S)$. Therefore, McConnell's relationship is generally expressed as

$$a_i = Q\rho_i^\pi/(2S) \tag{2}$$

where a_i and ρ_i^π denote the isotropic hfcc of the α-proton of the *i*th carbon atom and the π spin density of the *i*th carbon atom, respectively. The relation between a_i of quartet and quintet states is given as follows.

$$a_i(\text{quartet}) = \frac{4}{3}\frac{\rho_i^\pi(\text{quartet})}{\rho_i^\pi(\text{quintet})}a_i(\text{quintet}) \tag{3}$$

From eq 3 the hfcc of the protons of the anion will be $^2/_3$ of those of the quintet molecule if the excess electron occupies one of the two π-SOMOs (π-anion), whereas they will be $^4/_3$ of those of the quintet if the electron occupies the n-orbital (n-anion).

The hfcc of all the 14 protons of the neutral quintet *m*-PBPM have been fully analyzed using single-crystal samples to reveal that the isotropic hfcc are in the range −8.0 to +3.6 MHz and that the magnitude of the anisotropic part is within ≈4 MHz.[19] Therefore, the isotropic hfcc of the π-anion will be in the range −5.3 to +2.4 MHz, and the maximum (negative) value of the hfcc including the anisotropy will be ≈−8 MHz. In the case of the n-anion the isotropic part will span a range −11 to +5 MHz.

In all the four observed ENDOR spectra of the quartet anion, the maximum absolute values of the hfcc are less than 10 MHz and most of the intensive signals are within a few MHz around ν_n as is seen from Figure 3. The orientations of the anion, which were pumped in the ENDOR measurements, correspond to the *X*- and *Y*-canonical axes and to the direction of $\theta \approx 38°$ for the extra line[27] (see Figure 2). Although the hfcc of the *Z*-direction could not be determined due to the feebleness of the ESR intensity, the result of the observed spectra from the three different directions indicates that the isotropic component decreases upon charging, which leads to the conclusion that the excess electron occupies most probably the π-orbital.

4. ESR Spectrum of the ^{13}C Substituted Isotopomer. When the excess electron in the anion occupies the π-orbital, the spin density of the n-orbital should remain essentially the same as that of the neutral quintet *m*-PBPM and the two divalent carbon atoms in the anion will have nearly the same isotropic hfcc. In order to see whether this is the case or not, we have prepared an isotopomer in which one of the two divalent carbon atoms is substituted by ^{13}C. All the canonical peaks and the off-axis extra line were broadened by the unresolved hyperfine splitting due to ^{13}C. The *Y*-axis canonical peak at ≈200 mT of the ^{13}C substituted isotopomer appears less acute and bell-shaped with a larger line width than that of the unsubstituted isotopomer (see Figure 4a).

According to the above discussion on the π-anion the spin density at both divalent carbon atoms, ^{12}C and ^{13}C, should be nearly the same. Therefore, the observed peak should split into a doublet due to the hyperfine splitting of the single ^{13}C. This is indicated in the left pattern of Figure 4b by the two dotted components with an assumed hyperfine splitting of 3.0 mT. On the other hand, if the excess electron resides in the *n*-orbital, the spin density at one of the two divalent carbon atoms with a closed-shell structure will be 0 whether the atom is ^{12}C or ^{13}C and the density at the other atom with an open-shell structure will be essentially the same as the quintet *m*-PBPM whose hfcc of the divalent ^{13}C atom is known to be ≈3.5 mT.[30] Therefore, in this case of the *n*-anion the observed peak should comprise, with an equal intensity, a singlet and a doublet. In the right pattern of Figure 4b a singlet and the two components of a doublet are shown in dotted lines, where the hyperfine splitting of the doublet is assumed to be 3.0 mT in conformity with the left pattern of Figure 4b. The integrated intensity of the singlet is the same as that of the doublet, and they are halved relative to the integrated intensity of the doublet in the case of the π-anion above. The observed peak coincides with the former case and not with the latter case, which reinforces the conclusion of the previous subsection that

(28) Teki, Y.; Takui, T.; Itoh, K. To be published.
(29) Rose, M. E. *Elementary Theory of Angular Momentum*; John Wiley & Sons: New York, 1957.
(30) Teki, Y. et al. To be published.

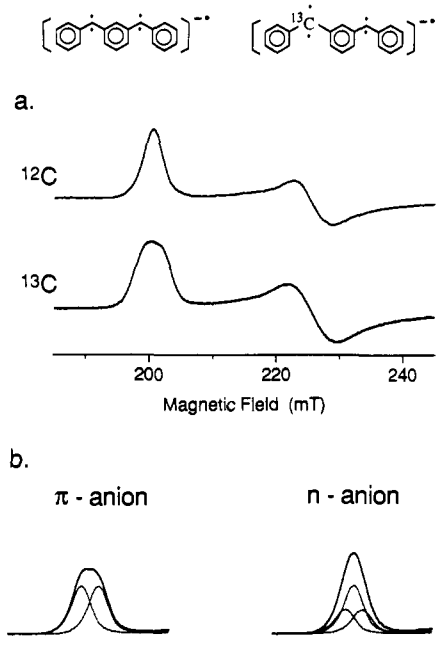

Figure 4. (a) ESR spectrum of ^{13}C substituted *m*-PBPM$^{\bullet-}$ in which one of the two divalent carbon atoms was labeled by ^{13}C. The spectrum of the unsubstituted is also shown for comparison. (b) Synthetic peaks consisting of ^{12}C isotopomers. Left, the one corresponding to the spectrum of the π-anion of ^{13}C isotopomer which has a single ^{13}C hfcc of 3.0 mT. Right, the one corresponding to the spectrum of the n-anion of ^{13}C isotopomer which has ^{13}C hfcc of 0 mT and 3.0 mT.

the π-anion is favored over the n-anion. The anisotropic component of the hfcc is totally neglected in the analysis of the *Y*-axis canonical peak at ≈200 mT. However, because all the other *X*- and *Y*-axis canonical peaks can be regarded as comprising the two components with a separation of ≈3.0 mT, the isotropic part of the hfcc of the two divalent carbon atoms are considered to be approximately equal, which is consistent with the conclusion of the π-anion. The anisotropic component of the hfcc could not be analyzed because the hyperfine splittings were not resolved enough for the analysis.

Since an accurate hfcc cannot be obtained from the above argument based on the line shape of the ESR signal, we attempted to observe the ^{13}C-ENDOR signal. However, the signal to noise ratio was too small to detect the signal.

The isotropic hfcc of the divalent ^{13}C atom of the anion is close to that of the neutral *m*-PBPM, which is ≈3.5 mT,[30] whereas the isotropic hfcc of the divalent ^{13}C atom of diphenylmethylene (DPM) is reported as 173.3 MHz (6.184 mT).[31] Since the spin density of the n-orbital of DPM and *m*-PBPM is essentially the same, as relation similar to eq 3 predicts that the isotropic hfcc of the divalent ^{13}C atom of *m*-PBPM is $^1/_2$ of that of DPM, which agrees with the observation. Thus, the semiquantitative argument here works fine in the neutral systems. However, the isotropic hfcc of the anion of ≈3.0 mT does not agree with the estimation based on eq 3 which predicts that the hfcc of the anion should be $^4/_3$ of that of the neutral *m*-PBPM, i.e., ≈4.7 mT. Possible reasons for the discrepancy are the loss of the planarity and the change in the ratio of s–p mixing at the divalent carbon atoms upon charging. There is also the possibility of an effect of orbital expansions upon the electron attachment.

5. Molecular Conformation of *m*-PBPM$^{\bullet-}$. Since the fine structure parameters of the anion are now determined as D = +0.1200 cm^{-1} and $|E|$ = 0.0045 cm^{-1} [32] and the excess electron is in the π-orbital, we can discuss the molecular conformation of the anion by comparing the fine structure parameters with those of diphenylmethylene (DPM) and *m*-PBPM; a semiquantitative expression for the fine structure tensor is given by the superposition of the dominant one-center spin–spin interaction of n-π type at each divalent carbon atom.[13] Assuming that the one-center interaction can be represented by the fine structure tensor of DPM, we obtain[14b]

$$D_{ij} = [S(2S-1)]^{-1}\sum_k(\rho_k/\rho_{DPM})(U_k\cdot\mathbf{D}_{DPM}\cdot U_k^{-1})_{ij} \qquad i,j = X, Y, Z \quad (4)$$

where D_{ij} stands for the ij element of the fine structure tensor of the anion, the subscript k runs over all the divalent carbon atoms and $\mathbf{D}_{DPM}$ denotes the fine structure tensor of DPM represented in the principal axis system. The symbols ρ_k and ρ_{DPM} represent the spin density of the π-electron at the kth divalent carbon atom and that at the divalent carbon atom of DPM, respectively. The unitary matrix U_k transforms the molecule fixed axes to the principal axes of the one-center interaction tensor at the kth divalent carbon atom. Since a simple LCAO-MO calculation gives the spin densities of $\rho_{DPM} = {}^2/_5$ and $\rho_{m\text{-}PBPM} = 0.4040$, the ratio $\rho_{m\text{-}PBPM}/\rho_{DPM}$ can be regarded as unity. We must take into account the projection factor $[S(2S-1)]^{-1}$ which is 1 for the triplet DPM, $^1/_3$ for the quartet anion, and $^1/_6$ for the quintet *m*-PBPM. Since the excess electron of the anion occupies the π-orbital, the π-electron spin density will be reduced to $\rho_k \approx \rho_{m\text{-}PBPM}/2$.

If the conformation of the anion remains the same as that of the neutral *m*-PBPM, which is known to be conformation A,[13,19]

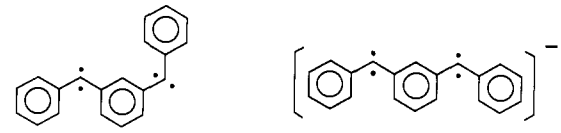

A B

the unitary matrices U_k's should be almost the same as those of the neutral *m*-PBPM. Noticing that the projection factor of the anion is twice as large as that of *m*-PBPM together with the relation of ρ_k(anion) ≈ $\rho_{m\text{-}PBPM}/2$, we find D_{ij}(anion) ≈ D_{ij}(*m*-PBPM). Thus, the fine structure parameters of the anion would have to be close to those of the neutral *m*-PBPM, i.e., D = +0.07131 cm^{-1} and $|E|$ = 0.01902 cm^{-1}.[1] However, the observed parameters of the anion are far from those of *m*-PBPM. The $|E/D|$ value for the anion, 0.038, which is a measure of the deviation from the axial symmetry of the tensor, is also quite different from that for *m*-PBPM, i.e., 0.2667.[1]

However, if the conformation of the anion is in a trans-trans type as depicted in conformation B, the two one-center interaction tensors at the divalent carbon atoms are roughly parallel so that the sum in eq 4, $\sum_k(\rho_k/\rho_{DPM})(U_k\cdot\mathbf{D}_{DPM}\cdot U_k^{-1})_{ij}$, will be close to $^1/_2 \times 2\mathbf{D}_{DPM} \approx \mathbf{D}_{DPM}$. Since the projection factor $[S(2S-1)]^{-1}$ is 1 for DPM and $^1/_3$ for the anion, the fine structure parameters of the anion will be about $^1/_3$ of those of DPM. The fine structure parameters of DPM are D = +0.40505 cm^{-1} and $|E|$ = 0.01918 cm^{-1} with the $|E/D|$ value being 0.04735.[31] From these values the parameters of the anion are estimated as $D \approx D(\text{DPM})/3$ = +0.135 cm^{-1}, $|E| \approx |E(\text{DPM})|/3$ = 0.0064 cm^{-1}, and $|E/D| \approx |E/D(\text{DPM})|$ = 0.047, which are close to the experimental values for the monoanion, D = +0.1200 cm^{-1}, $|E|$ = 0.0045 cm^{-1}, and $|E/D|$ = 0.038. It should be noted that the above argument is based upon the assumptions that the orbital interaction between the two singly occupied n-orbitals is negligibly small, and the two n-orbitals are nearly degenerate in both the asymmetric conformation A and symmetric B.

Using the fact that the fine structure tensor of aromatic polycarbenes can be approximated as the superposition of the one-center interaction at each divalent carbon atom and the π-electron spin density of the anion is about one-half of that of *m*-PBPM, the conformation of the anion is now suggested as to

(31) Brandon, R. W.; Closs, G. L.; Davoust, C. E.; Hutchison, C. A., Jr.; Kohler, B. E.; Silbey, R. *J. Chem. Phys.* **1965**, *43*, 2006–2016.

(32) The absolute values of D and E were determined by simulation in the previous work.[23]

(33) Higuchi, J. *J. Chem. Phys.* **1963**, *38*, 1237–1245. Higuchi, J. *J. Chem. Phys.* **1963**, *39*, 1847–1852.

be in a trans-trans type such as B.

Now a question arises as to why the anion of *m*-PBPM prefers a trans-trans conformation. This question of the difference in the molecular structure favored by the neutral species and by its anion is considered to be a crucial problem in spin chemistry. As far as we known,[13,14b,27] neutral high-spin molecules of a linear molecular struture often undergo thermally stimulated conformational changes such as phenyl ring flips,[13,14b] when generated by UV photolysis in solid, *without* the change in the spin multiplicity. As for the monoanion of *m*-PBPM formed by photolytic denitrogenation of the monoanion of 1,3-BDB, there may be chances in molecular structural changes during the whole series of reactions starting from the electron attachment to the parent 1,3-BDB. However, since there is little experimental information on the molecular structure of each stage of the reactions,[34] arguments on the spin-conversion process in relation to molecular structures are prohibitive at the moment. Appropriate molecular orbital calculations for charged high-spin molecules may shed light on this problem. A project along this line is now under way.

(34) The spin conversion process from singlet-state 1,3-BDB to quintet-state *m*-PBPM has been studied by time-resolved picosecond laser optical spectroscopy: T. Takui and K. Itoh, unpublished work.

Conclusion

From the present work it was determined that the ground state of the monoanion of *m*-PBPM is quartet. A theory suggesting the possibility of the reversal of the order of high- and low-spin states upon charging[22] is not substantiated in this system. From the ^{1}H-ENDOR measurements it is concluded that the excess electron resides on the nonbonding π-orbital. This result is compatible with the ESR measurement of the ^{13}C substituted isotopomer. The molecular conformation of the anion is suggested to be of a trans-trans type.

Acknowledgment. The Kyoto group is indebted to Professor Takashi Kawamura for this generosity in allowing us to use his ESR equipment. The Osaka group thanks both the Computer Center, Institute for Molecular Science, Okazaki National Research Institutes for the use of the HITAC M68OH computer and the Computer Center, Osaka City University. Spectral simulations were also carried out at the Data Processing Center of Kyoto University. The study was partially supported by Grants-in-Aid for Scientific Research on priority Areas (Grant Nos. 02205070, 02205102, and 04242103) and Grant-in-Aid for General Scientific Research (Grant Nos. 02453014 and 03640429) of the Ministry of Education, Science, and Culture in Japan.

Using Saturation–Recovery EPR To Measure Exchange Couplings in Proteins: Application to Ribonucleotide Reductase

Donald J. Hirsh,[†] Warren F. Beck,[†,‡] John B. Lynch,[§] Lawrence Que, Jr.,[§] and Gary W. Brudvig*,[†]

Contribution from the Departments of Chemistry, Yale University, 225 Prospect Street, New Haven, Connecticut 06511, and University of Minnesota, 207 Pleasant Street, S.E., Minneapolis, Minnesota 55455. *Received February 28, 1992*

Abstract: The stable tyrosine radical of ribonucleotide reductase (RNR) from *Escherichia coli*, Tyr 122 of the B2 subunit, exhibits single-exponential spin–lattice relaxation kinetics for $T \leq 16$ K and nonexponential spin–lattice relaxation kinetics at higher temperatures. Saturation–recovery transients of the tyrosine radical are analyzed using a model developed to treat the interaction of two paramagnets in a rigid lattice at a fixed distance apart but with a randon orientation in the static magnetic field. The model describes the spin–lattice relaxation of a radical in proximity to another paramagnetic site in terms of two isotropic or "scalar" rate constants and an orientation-dependent rate constant. The scalar rate constants arise from (1) intrinsic relaxation processes of the radical which exist in the absence of the other paramagnetic site and (2) a scalar-exchange-induced relaxation process arising from orbital overlap between the two paramagnetic sites. The orientation-dependent rate constant arises from a dipole–dipole-induced relaxation process. From simulations of the higher temperature saturation–recovery transients, we conclude that their nonexponential character arises from a dipole–dipole interaction with the diferric center of RNR. The tyrosine radical generated by UV photolysis of L-tyrosine in a borate glass is used as a model for the intrinsic spin–lattice relaxation rate of the tyrosine radical of ribonucleotide reductase. Comparison of the scalar rate constants derived from simulations of the saturation–recovery transients of the tyrosine radical of RNR with the single-exponential rate constants of the model tyrosine radical indicates scalar exchange is also a source of relaxation enhancement of the tyrosine radical of RNR at higher temperatures. We present a new method for determining the exchange coupling of the diferric center based on the temperature dependence of the scalar-exchange and dipolar rate constants. The Fe(III)–Fe(III) exchange coupling is estimated to be -94 ± 7 cm^{-1}. We also estimate an exchange coupling of $|0.0047 \pm 0.0003$ cm$^{-1}|$ between the diferric center and the tyrosine radical on the basis of the relative contributions of scalar-exchange and dipolar interactions to the spin–lattice relaxation and the distance between the two sites. The source of line broadening of the EPR signal of the tyrosine radical of RNR at temperatures greater than 75 K is discussed as well.

Introduction

The enzyme ribonucleotide reductase (RNR) catalyzes the reduction of ribonucleotides to the corresponding deoxyribonucleotides. RNR from *Escherichia coli* consists of two subunits, B1 and B2, both of which are homodimers.[1] The B1 subunit binds the allosteric effectors and the substrate ribonucleotides, but both B1 and B2 contribute to the active site of the enzyme. Each polypeptide of the B2 subunit of RNR from *E. coli* contains one non-heme μ-oxo-μ-carboxylato-bridged dinuclear Fe(III) com-

[†] Yale University.
[‡] Current address: Department of Chemistry, Vanderbilt University, Nashville, TN 37235.
[§] University of Minnesota.

(1) Atkin, C. L.; Thelander, L.; Reichard, P.; Lang, G. *J. Biol. Chem.* **1973**, *248*, 7464–7472.

0002-7863/92/1514-7475$03.00/0